



# Fra-2/AP-1 regulates melanoma cell metastasis by downregulating Fam212b

Guang-Liang Chen<sup>1,2,3</sup> · Rui Li<sup>2,4</sup> · Xiao-Xiang Chen<sup>4</sup> · Juan Wang<sup>4</sup> · Shan Cao<sup>2,4</sup> · Rui Song<sup>2,4</sup> · Ming-Chun Zhao<sup>5</sup> · Li-Ming Li<sup>6</sup> · Nicole Hannemann<sup>2</sup> · Georg Schett<sup>2</sup> · Cheng Qian<sup>7</sup> · Aline Bozec<sup>2</sup>

Received: 26 February 2019 / Revised: 19 October 2020 / Accepted: 23 October 2020 / Published online: 13 November 2020  
© The Author(s), under exclusive licence to ADMC Associazione Differenziamento e Morte Cellulare 2020

## Abstract

Metastatic melanoma remains a challenging disease. Understanding the molecular mechanisms how melanoma becomes metastatic is therefore of interest. Herein we show that downregulation of the AP-1 transcription factor member Fra-2 in melanoma cells is associated with an aggressive melanoma phenotype in vitro and in vivo. In vitro, Fra-2 knockdown in melanoma cells promoted cell migration and invasion associated with increased Snail-1, Twist-1/2, and matrix metalloproteinase-2 (MMP-2) expression. In vivo, Fra-2 knockdown in a melanoma cell line led to increased metastasis into the lungs and liver. The increased metastatic potential of Fra-2 knockdown melanoma cells was likely due to an accelerated cell cycle transition and increased tissue angiogenesis. Using Fra-2 knockdown cell lines microarray analysis, we identified the protein Fam212b (family with sequence similarity 212 member B) as a downstream target of Fra-2. By additional knockdown of Fam212b in Fra-2 mutant cells, we mitigated the cell migration, invasion, and cell cycle transition phenotype induced by Fra-2 knockdown. Furthermore, Fam212b overexpression enhanced  $\beta$ -catenin pathway. Finally, Fam212b expression is correlated with increased melanoma metastasis and poor clinical outcomes in human patients. In summary, these findings reveal the Fra-2-Fam212b axis as a new pathway of melanoma metastasis, which can be in the future used as potential marker of the metastatic properties of melanoma.

---

These authors contributed equally: Guang-Liang Chen, Rui Li, Xiao-Xiang Chen

---

These authors jointly supervised this work: Cheng Qian, Aline Bozec

---

Edited by S. Fulda

---

**Supplementary information** The online version of this article (<https://doi.org/10.1038/s41418-020-00660-4>) contains supplementary material, which is available to authorized users.

---

✉ Aline Bozec  
aline.bozec@uk-erlangen.de

- <sup>1</sup> Department of Medical Oncology, Fudan University Shanghai Cancer Center, Shanghai, China
- <sup>2</sup> Department of Internal Medicine 3-Rheumatology and Immunology, Friedrich-Alexander-University Erlangen-Nürnberg (FAU), Universitätsklinikum Erlangen, Erlangen, Germany
- <sup>3</sup> Department of Oncology, Shanghai Medical College, Fudan University, Shanghai, China

## Background

Clinical outcomes of patients with metastatic melanoma remain poor [1]. Although a subset of patients with metastatic melanoma benefit from new treatments [2], the presence of metastasis is associated with poorer prognosis in melanoma patients. Metastasis is a multistep process that involves cancer cell detachment, migration, colonization, and survival in distant organs [3, 4]. The current understanding of the pathways influencing the metastatic behavior is yet incomplete.

- <sup>4</sup> Department of Rheumatology, Renji Hospital, Affiliated to Shanghai Jiao Tong University, School of Medicine, Shanghai, China
- <sup>5</sup> Department of Pathology, Guilin People's Hospital, Guilin, Guangxi, China
- <sup>6</sup> Department of Pediatric Surgery, Guigang People's Hospital, Guigang, Guangxi, China
- <sup>7</sup> Department of Thoracic Surgery, Zhongshan Hospital, Fudan University, Shanghai, China

Activator protein 1 (AP-1) transcription factors form dimers containing members from the Jun, Fos, activating transcription factor (ATF), and Maf protein families [5]. They have oncogenic or anti-oncogenic functions and are involved in multiple cell processes, including tumor invasion [5]. Dysregulation of AP-1 proteins, such as Fos-like 1 (Fra-1 or Fos11), c-Jun, JunB, and c-Fos in melanoma has already been characterized [6]. For example, decreased Fra-1 expression in melanoma cells leads to sensitivity to kinase inhibitors, including vemurafenib, crizotinib, and erlotinib [7]. Fra-1, together with the B-Raf proto-oncogene (BRAF) pathway, regulates epithelial–mesenchymal transition (EMT) by activating a tight network of transcription factors [3]. Similarly, c-Jun expression induces EMT-like phenotypic changes and BRAF inhibitor resistance in melanoma [8]. Moreover, Annelien et al. identified AP-1 transcription factors as potential regulators of melanoma cell invasion [9].

Although several reports have described the role of Fos-like antigen 2 (Fra-2 or Fos12) in neural tumor cells [10], breast cancer [11, 12], and lymphomas [13], little is known about its role in melanoma. Fra-2 functions in human melanoma by inducing major histocompatibility complex (MHC) class I antigen or Fas expression, leading to a reduction in intracellular reactive oxygen species (ROS) levels and inhibition of anchorage-independent growth [14]. These abovementioned studies led us to investigate the role of Fra-2 in more details in melanoma cells.

Fam212b (family with sequence similarity 212 member B), which is also designated as INKA2, is expressed at high levels in the nervous system and may be involved in multiple actin-driven processes, including cell migration and the establishment of neuronal polarity [15]. Fam212b inhibits by binding the serine/threonine-protein kinase PAK4 (P21-activated kinase 4) in a substrate-like manner. According to the recent report by Yun et al., PAK4 regulates melanoma development by controlling cAMP-response element (CRE)-binding protein (CREB), microphthalmia-associated transcription factor (MITF), and  $\beta$ -Catenin signaling [16]. However, there is no report on the role of Fam212b in melanoma cells.

In the present study, we first analyzed Fra-2 expression in melanoma samples from several public databases, including Gene Expression Omnibus (GEO) and The Cancer Genome Atlas (TCGA). We also characterized the functional role of Fra-2 in murine melanoma cell lines using in vitro and in vivo loss of function experiments and validated our findings in two human melanoma cell lines. Mechanistically, we show that Fra-2 mediated effects on the migration and invasion phenotype of melanoma cells depend on Fam212b, which regulates the  $\beta$ -Catenin signaling. Finally, we show that Fam212b expression correlates with increased melanoma metastasis in humans and

may therefore represent a new marker for melanoma cells undergoing metastasis.

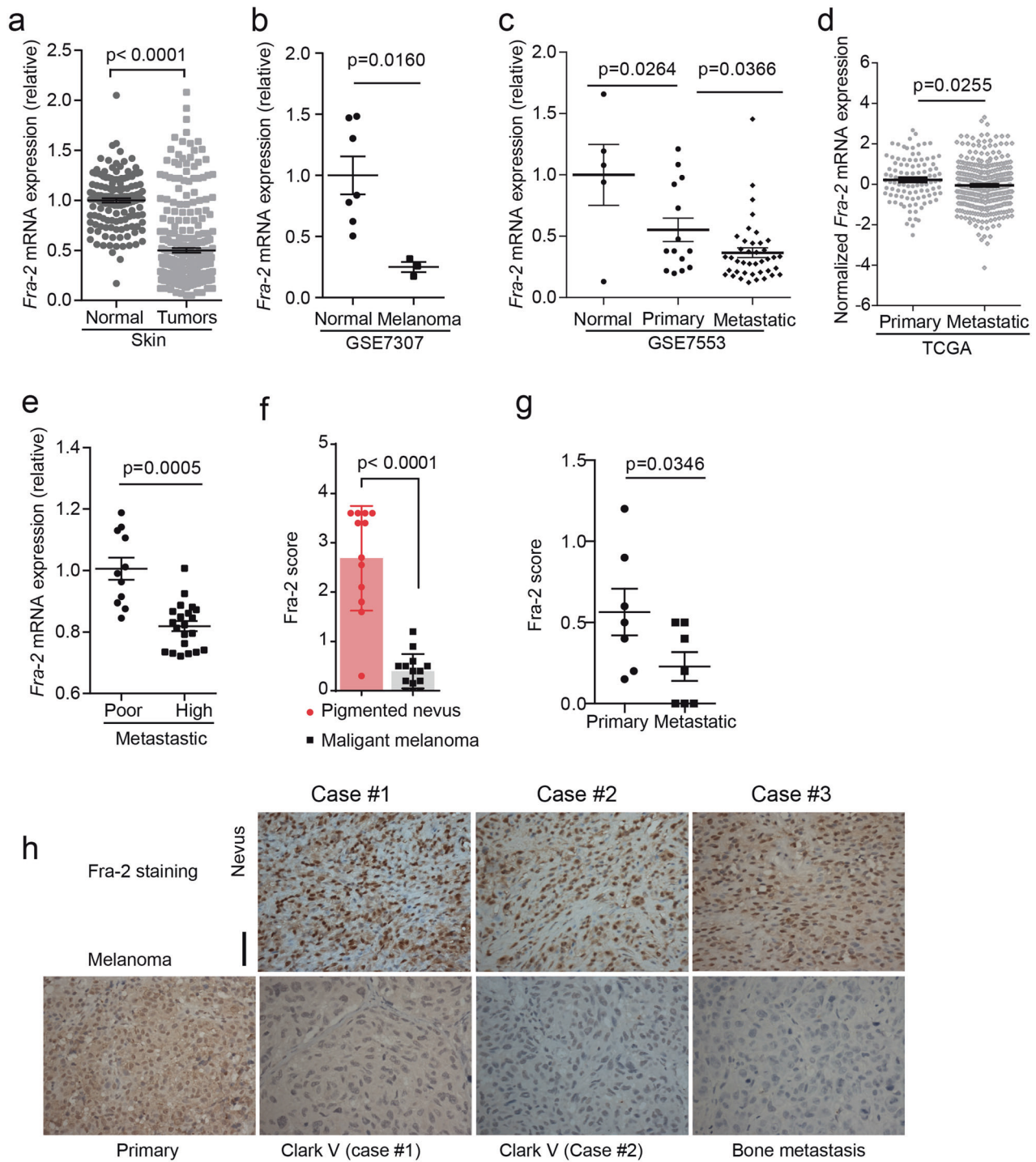
## Results

### Fra-2 is downregulated in patients with metastatic melanoma

We initially analyzed the expression of Fra-2 transcripts in normal skin and skin tumors by searching the web-accessible Gene Expression across Normal and Tumor tissue (GENT) database [17], which includes normalized data obtained from GEO databases [18]. As shown in Fig. 1a, patients with skin tumors displayed significantly decreased levels of *Fra-2* mRNA compared to normal skin samples. As melanoma represents one of the most aggressive forms of skin cancer [19], we analyzed three independent clinical data sets (GSE7307, GSE7553, GSE3189) [20, 21], which all revealed that *Fra-2* mRNA levels were significantly lower in melanoma samples than in normal skin or in naevus tissues (Fig. 1b, c and Supplementary Fig. 1a). Moreover, *Fra-2* mRNA levels were significantly reduced in patients with metastatic melanoma compared to patients with primary melanoma (Fig. 1c, d and Supplementary Fig. 1b). Accordingly, *Fra-2* mRNA levels were significantly lower in highly metastatic melanoma cell lines (GSE7929) [22, 23] than in human A375 melanoma cell lines that are poorly metastatic (Fig. 1e). Accordingly, immunohistochemical examination of Fra-2 expression in skin samples from a cohort of patients with melanoma ( $n = 14$ ) showed significantly lower protein levels than patients suffering from benign naevus ( $n = 12$ ) (Fig. 1f). Furthermore, patients with metastatic melanoma had an even lower Fra-2 expression than patients with primary melanoma (Fig. 1g, h). In accordance, we also detected lower Fra-2 protein levels in murine B16-F10 cells, which are known to be highly metastatic [24, 25], than in B16-F0 cells (Supplementary Fig. 1c). However, *Fra-2* mRNA levels were not correlated with melanoma disease stage or chemotherapy response rate (Supplementary Fig. 1d). Overall, these data suggested that Fra-2 expression is downregulated in metastatic melanoma cell lines and in patients with metastatic melanoma.

### Fra-2 knockdown induced an aggressive phenotype in melanoma

To investigate the functions of Fra-2 in melanoma cells, Fra-2 expression was knocked down in murine B16-F0 melanoma cells by transfection with shRNA against Fra-2 (Fig. 2a and Supplementary Fig. 2a), without affecting the expression of other AP-1 transcription factors such as c-Fos,



FosB, Fra-1, c-Jun, and JunD (Supplementary Fig. 2b). Two B16-F0 cell clones with stable Fra-2 knockdown (shFra-2-E4 and shFra-2-F4) were selected and further analyzed for their biological behaviors in vitro (Fig. 2a). According to the results from wound healing assays (Fig. 2b) and transwell migration assays (Fig. 2c), Fra-2 knockdown (Fra-2KD) increased the migration of melanoma cells compared to control B16-F0 cells transfected with scramble shRNA.

In addition, a greater number of Fra-2KD cells migrated through the basement membrane extract (BME)-coated membranes in transwell inserts than the B16-F0 control cells (Fig. 2d), indicating that Fra-2KD increased melanoma cell invasion. Despite no change in *Cspg4*, *Pdgfa*, and *VEGfa*, cell migration-related gene expression profiling revealed increased expression of *C-X-C motif chemokine receptor 3 (CXCR3)*, *sine oculis homeobox homolog 1*

◀ **Fig. 1 Decreased Fra-2 expression is associated with aggressive malignant melanoma phenotypes in humans and mice.** **a** Patterns of *Fra-2* mRNA expression in human skin tumors ( $n = 302$ ) and normal skin tissue ( $n = 142$ ) were analyzed using GENT. **b** Microarray analysis of *Fra-2* mRNA levels in normal tissues ( $n = 7$ ) compared with tissues from patients with melanoma ( $n = 3$ ) (GSE7307). **c** Microarray analysis of *Fra-2* mRNA levels in normal tissues ( $n = 5$ ) compared with non-metastatic cutaneous tumors ( $n = 14$ ) and metastatic melanoma ( $n = 40$ ) (GSE7553). **d** *Fra-2* mRNA levels obtained from TCGA SKCM samples with primary tumors ( $n = 103$ ) and metastatic tumors ( $n = 369$ ). Normalized *Fra-2* mRNA levels were generated using a Z-score method. **e** Microarray analysis of *Fra-2* mRNA expression levels in human A375 melanoma cell lines that showed low ( $n = 11$ ) and high ( $n = 21$ ) metastatic abilities in the lungs of immunodeficient mice that were injected s.c. or i.v. (GSE7929). **f** Fra-2 scores were calculated by multiplying the nuclear intensity of Fra-2 staining by the percentage of positively stained cells. **g** Fra-2 scores were evaluated in patients with primary ( $n = 7$ ) or metastatic melanoma ( $n = 7$ ). **h** Representative immunohistochemical staining for Fra-2 in paraffin-embedded samples from patients with pigmented nevus ( $n = 12$ ) and melanoma ( $n = 14$ ). Scale bar, 50  $\mu\text{m}$ . Graphs present the mean values for each group and error bars represent the s.e.m.  $P < 0.05$  was considered statistically significant using unpaired Student's *t*-tests (two-tailed) for single comparisons.

(*Six1*), *C-C motif chemokine ligand 5 (CCL5)*, *S100 calcium-binding protein A6 (S100A6)* and decreased *AVL9 cell migration associated (Avl9)* genes in Fra-2KD melanoma cells (Fig. 2e). Moreover, Western blot analysis of EMT markers revealed that Fra-2KD increased the levels of Snail family transcriptional repressor 1 (Snail-1), Twist family basic helix-loop-helix (BHLH) transcription factor 1/2 (Twist-1/2) and matrix metalloproteinase-2 (MMP-2) proteins, whereas it decreased the levels of E-cadherin and N-cadherin proteins and do not alter MMP9 or Vimentin (Fig. 2f). To rule out off-target or cell-specific effects, knockdown of Fra-2 with two different shRNA was performed in murine B16-F0 cells (Supplementary Fig. 1c–e) as well as in two human A375 or A875 melanoma cell lines (Supplementary Fig. 1f–i), resulting in a similar invasive and aggressive phenotype, as shown by mRNA expression and protein level of EMT-related markers. Indeed, analyses of the morphology of Fra-2KD melanoma cells showed a dendritic morphology compared to control cells (Supplementary Fig. 3a).

Furthermore, flow cytometry analysis of the cell cycle showed that Fra-2KD promoted the G0 phase to G1/S phase transition (Supplementary Fig. 3b), which was associated with an increased expression of cyclin D1 (CCND1) (Supplementary Fig. 3c). Using the cell counting kit-8 (CCK-8 assay), we showed that Fra-2KD promoted melanoma cell proliferation to a greater extent than control cells (Supplementary Fig. 3d). Moreover, Fra-2KD increased the proliferation rate of the human A375 cell line but not of the A875 melanoma cells (Supplementary Fig. 3e). In contrast, no changes in early (Annexin V + PI<sup>-</sup>) and late apoptotic cells (Annexin V + PI<sup>+</sup>) were observed (Supplementary

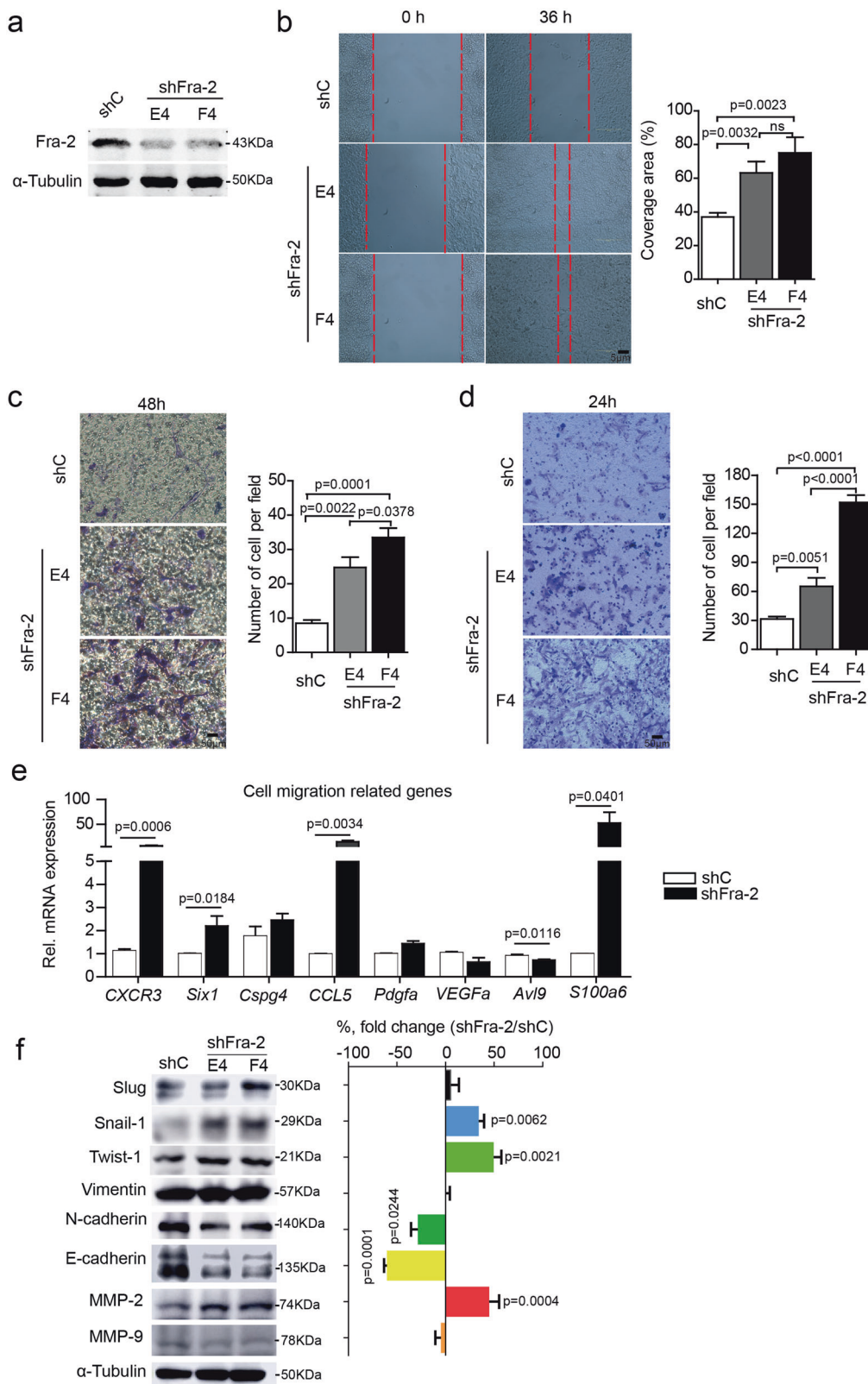
Fig. 3f). Taking together, these data suggested that decreased Fra-2 expression in melanoma cells promoted an invasive and aggressive phenotype and increased cell proliferation by accelerating cell cycle transitions.

### Decreased Fra-2 expression in melanoma cells induced metastatic behavior in melanoma cells

We performed intravenous (i.v.) and intracardial (i.c.) injections of shFra-2-F4 and control (ShC) melanoma cells into immunocompetent C57BL/6 mice ( $n = 8$  for each group) to test whether Fra-2 knockdown promoted melanoma metastasis in vivo. As shown in Fig. 3a, b, the number of nodules in the lungs and liver was significantly increased after i.v. and i.c. injections of Fra-2 knockdown cells, respectively. Immunohistochemical staining for CD34 in metastatic tumor foci in the liver revealed increased angiogenesis in mice injected with Fra-2 KD melanoma cells (Fig. 3c). Moreover, the increased number of tumor colonies in mice injected with Fra-2KD melanoma cells correlated with an increased percentage of Ki67-expressing tumor cells (Fig. 3d). Thus, Fra-2KD in melanoma cells promoted angiogenesis and proliferation of the tumor cells in vivo. No difference was detected for *Pdgfa*, *Stb1*, and *Timp3*. But according to the increased angiogenesis in Fra-2 KD cells, increased expression of angiogenesis markers, such as *angiopoietin 4 (Ang4)*, *angiopoietin-like 4 (Angptl4)*, *laminin subunit gamma 2 (Lamc2)*, *inhibitor of DNA binding 1 (Id1)*, *HLH protein* and *vascular endothelial growth factor C (Vegfc)* mRNA levels (Fig. 4e), and cell cycle transition-related genes, such as *CyclinD1 (Ccnd1)*, *cyclin-dependent kinase inhibitor 1 A (Cdkn1a)*, and *polo-like kinase 2 (Plk2)* were detected (Fig. 3f), in mice injected by Fra-2KD melanoma cells compared to control cells. Subcutaneous tumors derived from Fra-2KD melanoma cells exhibited a similar growth rate than control cells also in nude mice (Supplementary Fig. 4a). Thus, downregulation of Fra-2 promotes melanoma cells metastasis in vivo.

### Profiling of Fra-2-regulated genes in murine melanoma cells

To delineate the molecular targets of Fra-2 in melanoma cells, we performed a mouse transcriptome assay of Fra-2KD B16-F0 melanoma cells. Among the 41,174 genes tested, 732 genes were altered in Fra-2 knockdown B16-F0 melanoma cells compared to B16-F0 control cells ( $p < 0.05$ ) (Supplementary Table 4). After selecting genes with an expression value greater than 7 and an alteration of expression greater than a threefold change, only 22 genes remained (Fig. 4a); 9 genes were down- and 13 genes upregulated in Fra-2KD melanoma cells (Fig. 4a). Next, the



enrichment of these differentially expressed genes was assessed using Gene Ontology (GO) [26] and Kyoto Encyclopedia of Genes and Genomes (KEGG) pathway

[27] analyses. The top 10 Fra-2-regulated genes were part of the cellular components, cytoplasm, molecular function, G-protein coupled receptor activity, and biological processes

**◀ Fig. 2 Fra-2 knockdown in melanoma cells induces cell migration, invasion, and EMT processes in vitro.** **a** Western blot analysis of the Fra-2 protein in B16-F0 cells transfected with a scrambled shRNA (ShC) and 2 clones transfected with shRNAs against Fra-2 (E4 and F4). **b** Representative images of scratch assays and quantification of the percentage of mobility of 2 B16-F0 cell clones transfected with shRNAs against Fra-2 (E4 and F4) and B16-F0 cells transfected with the control vector (Bars: 5  $\mu$ m). **c** Representative images of crystal violet staining and quantification of the numbers of melanoma cells crossing the transwell membrane, which represents cell migration (Bars: 50  $\mu$ m). **d** Representative images of crystal violet staining and quantification of crystal violet-positive melanoma cells that crossed the basement membrane extract (BME)-coated transwell chamber, which represents cell invasion (Bars: 50  $\mu$ m). **e** Quantitative PCR analyses of cell migration-related genes in control B16 cells and the 2 Fra-2 KD B16 cell clones (E4 and F4). **f** Western blot analysis of epithelial-mesenchymal transition (EMT) markers in control B16 cells and the 2 Fra-2 KD B16-F0 cell clones (E4 and F4). Three independent blots for Snail-1 and Twist-1/2; two independent blots were made for N-cadherin, E-cadherin, Slug, MMP2, MMP-9 and vimentin. At least three independent blots were made for  $\alpha$ -Tubulin. These blots were stripped and probed according to manufacturer's instructions. No bands represent the same blot. The quantification of the band intensity was performed using ImageJ software. Graphs present the means for each group and error bars represent the s.e.m. Representative data from 3 independent experiments are shown.  $P < 0.05$  was considered statistically significant using unpaired Student's *t*-tests (two-tailed) for single comparisons.

(Fig. 4b). Interestingly, the top 5 differentially expressed genes were involved in the process of olfactory transduction, proteasome function, hypoxia-inducible factor 1 (HIF-1) signaling pathway, lysosomal function, and the cell cycle (Fig. 4c). Next, we validated the expression of Fra-2-regulated genes identified from the microarray by quantitative PCR. Indeed, the expression of *endoplasmic reticulum oxidoreductase 1 alpha (Ero1A)*, *clathrin adapter protein (Dab2)*, *dachshund family transcription factor 1 (Dach1)*, *tensin 1 (Tns1)*, *Fam212b*, *S100A6*, and *thioredoxin interacting protein (Txnip)* (Fig. 4d), as well as the genes shown in Fig. 4e and f, was consistent with the changes observed in the microarray experiment. In addition, HIF-1 $\alpha$  expression was increased in Fra-2 KD melanoma cells compared to the control cells (Supplementary Fig. 5a).

### Fra-2 knockdown-induced cell migration and invasion of melanoma depended on Fam212b expression

To delineate the molecular mechanism by which Fra-2 regulates cell mobility and migration in melanoma, we focused on Fam212b (or Inka2, Corf183), because it was one of the most deregulated gene in our microarray, and it is involved in multiple actin-driven processes [15]. Indeed, levels of the *Fam212b* mRNA (Fig. 4d) and protein (Fig. 5a) were strongly increased in Fra-2KD melanoma cells compared to control melanoma cells. Fam212b, like Fam212a (Inka1), was previously described as inhibitor of

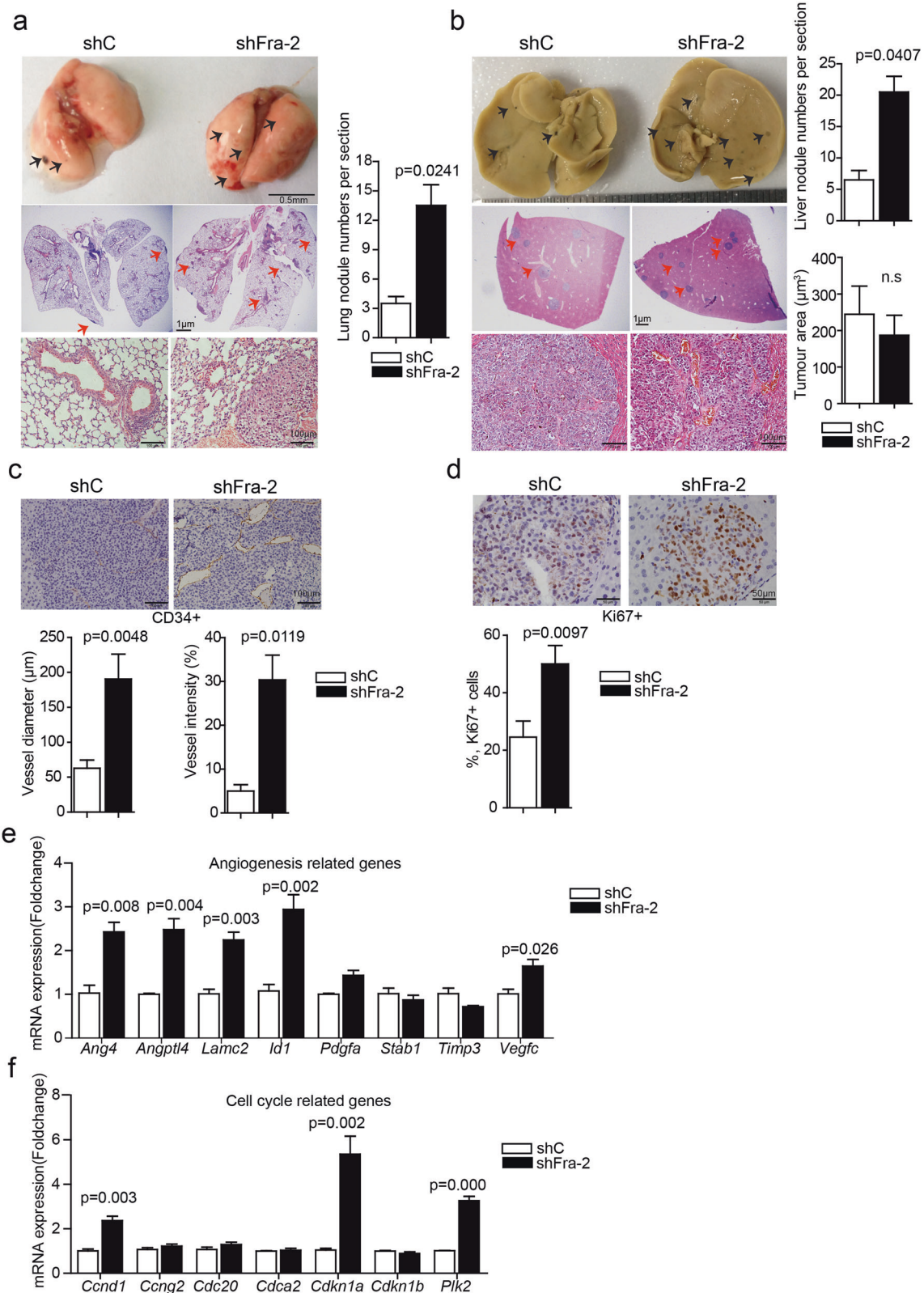
the serine/threonine kinase PAK4 in mammalian cells [28]. Therefore, we hypothesized that Fam212b may be a direct target gene of Fra-2 in melanoma cells. In support of this hypothesis, chromatin immunoprecipitation (ChIP) experiments showed that Fra-2 directly bound to 7 AP-1 binding site in -3650, -2974, -2134, -1818, -1583, -1249, and -1013bp *Fam212b* promoter in B16-F0 melanoma cells. No other AP-1 proteins tested bind to *Fam212b* promoter in Fra-2 KD cells. However, on the -2134bp and -1818bp, JunD binds only when Fra-2 is expressed, suggesting a possible cooperation between Fra-2 and JunD on *Fam212b* promoter (Fig. 5b). Next, we determined the *Fam212b* functions downstream of Fra-2 by knocking down *Fam212b* expression in melanoma cells that were already deficient in Fra-2. Indeed, transfection of specific siRNA sequences targeting *Fam212b* in Fra-2KD melanoma cells rescued pathological B16-F0 cell migration in wound healing assays (Fig. 5c) and B16-F0 cell invasion in trans-well invasion assays (Fig. 5d). Moreover, *Fam212b* knockdown restored the levels of Snail-1, E-cadherin, Twist-1/2, and MMP-2 proteins (Fig. 5e) as well as the levels of HIF1 $\alpha$  (Fig. 5f). As shown in Fig. 5g–i, *Ang4*, *Angptl4*, *Lamc2*, *Plk2*, *Id1*, *Vegfc*, *Ccnd1*, *Cdkn1a*, and *S100a6* mRNAs, that were altered in Fra-2 KD melanoma cells, are reduced in double KD cells. Moreover, *Fam212b* overexpression increased cell mobility and invasion in human A375 or A875 melanoma cells (Supplementary Fig. 5b–e), by inducing  $\beta$ -catenin signaling, Snail-1 or Zeb-1 mRNA and protein levels and inhibiting PAK4 phosphorylation (Supplementary Fig. 5f–i). These data strongly suggest that *Fam212b* transcription is regulated by Fra-2 and that *Fam212b* mediates the effects of Fra-2 on melanoma cell migration and invasion.

### Fam212b as biomarker that predicted poor clinical outcomes in patients with melanoma

We calculated the 5-year survival rate based on *Fam212b* mRNA levels in the SKCM dataset from TCGA to investigate whether *Fam212b* could represent a novel biomarker for melanoma metastasis. Interestingly, patients who expressed low levels of *Fam212b* in melanoma cells had a better prognosis than patients with high *Fam212b* expression ( $p = 0.0016$ ) (Fig. 6a). Based on results obtained from the same dataset, EMT gene scores were positively correlated with *Fam212b* mRNA expression ( $r^2 = 0.0437$ ,  $p < 0.0001$ ) (Fig. 6b), suggesting that *Fam212b* expression is associated with the expression of cancer metastasis-related genes in melanoma. Moreover, in the TCGA SKCM dataset, *Fam212b* mRNA levels were positively correlated with the expression of angiogenesis-related genes, such as *VEGFA* and *kinase insert domain receptor (KDR)* (Fig. 6c and Supplementary Fig. 6d). *Fam212b* was also positively

correlated with the mRNA levels of cell cycle transition-related genes, such as *Plk2*, *CDKN2B*, and *CDK6* (Fig. 6d and Supplementary Fig. 6e, f).

Similar to *Fra-2*, no correlation between *Fam212b* mRNA levels and tumor stage was observed in biopsies from melanoma patients (Supplementary Fig. 6g) and no



◀ **Fig. 3 Fra-2 knockdown in melanoma cells increased lung and liver metastases in mice in vivo.** Representative macrograph and micrograph images of mouse lungs (a) or liver (b) at day 12 after tail vein injection or day 14 after i.c. injection of Fra-2 KD or control B16-F0 cells. Quantification of metastatic tumor nodule numbers and metastatic tumor nodule areas in mouse lungs and livers ( $n = 8$  per group). Scale bar, upper panel, 0.5 mm; middle panel, 1  $\mu\text{m}$ ; lower panel, 100  $\mu\text{m}$ . c Immunohistochemical staining and quantification of the number of CD34-positive cells and vessels in metastatic foci in the liver tissues shown in (b). Scale bar, 100  $\mu\text{m}$ . d Immunohistochemical staining and quantification of Ki67-positive cells in the metastatic foci in the liver tissues shown in (b). Scale bar, 50  $\mu\text{m}$ . Quantitative PCR analyses of angiogenesis-related genes (e) and cell cycle transition-related genes (f) in Fra-2 KD and control B16-F0 cells. Graphs present the means for each group and error bars represent the s.e.m.  $P < 0.05$  was considered statistically significant using unpaired Student's  $t$ -tests (two-tailed) for single comparisons.

difference in Fam212b mRNA expression was detected between primary and metastatic samples (Supplementary Fig. 6h). However, Fam212b protein was ascertained by immuno-histochemical staining in a tissue arrays containing samples from patients with benign naevus, primary melanoma, and melanoma with lymph node metastasis. Indeed, Fam212b expression was highest in melanoma lymph node metastasis, significantly lower in primary melanoma and lowest in benign naevi (Fig. 6e, f). Taking together, our data suggested that Fam212b expression in melanoma cells could serve as a clinical biomarker for metastasis.

## Discussion

Metastatic melanoma remains a challenging disease. AP-1 family members Fra-1 and c-Jun have been investigated in melanoma [3, 29], while so far little is known about the role of Fra-2. We show that downregulation of Fra-2 increases the metastatic potential of melanoma cells by upregulation of Fam212b. Analyses of clinical datasets and expression analysis identified Fam212b as a biomarker for patients with metastatic melanoma.

The expression pattern of Fra-2 in melanoma cells is distinct from Fra-1, JunB, or c-Fos, but similar to c-Jun [3, 30]. However, similar to Fra-1, Fra-2 expression is also upregulated by *BRAF* mutations and functions downstream of the ERK1/2 pathway in melanoma cells [3]. Interestingly, inhibition of the *BRAF* pathway drives a metastatic switch in melanoma [31]. The decrease in Fra-2 expression induced by inhibition of the *BRAF* pathway may partially regulate this metastatic switch process. Interestingly, the AKT inhibitor MK-2206, which is currently being evaluated in phase 1 clinical trials as a treatment for melanoma (NCT01480154), increased Fra-2 expression in A375 and SK-MeL-1 cells, suggesting that Fra-2 and its key

downstream molecules may be also potential targets for the treatment of melanoma [32].

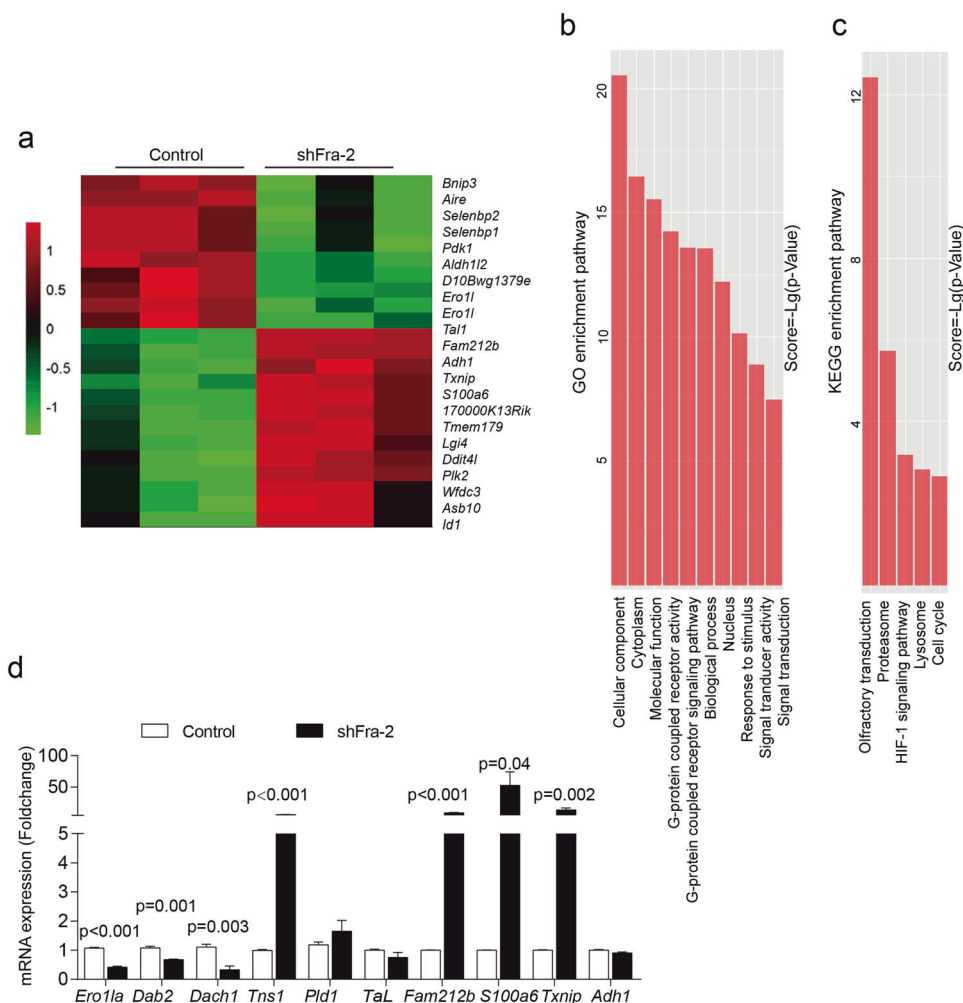
Fra-2 overexpression has been previously reported in several cancers, including breast cancer, non-small cell lung cancer, T-cell lymphomas, and lingual squamous cell carcinoma, which are associated with metastatic property by inducing cell proliferation, mobility, or invasion [13, 33–36]. In contrast, in the current study Fra-2 downregulation promoted melanoma cell proliferation, migration, and invasion in vitro and in vivo, suggesting that the role of Fra-2 in cell proliferation, migration, and invasion are heterogeneous among different tumor types [37]. Decreased Fra-2 expression is associated with increased expression of EMT markers, cell cycle transition- and angiogenesis-related genes in melanoma in vitro and/or in vivo. Accordingly, Fra-2 induction by resveratrol inhibited human melanoma cell growth in vitro [14]. Moreover, our data suggested that Fra-2 knockdown promotes the expression of HIF-1 $\alpha$ , which has been shown to activate the SRC non-receptor tyrosine kinase proto-oncogene, to promote melanoma metastases [38]. This result also confirmed our previous findings that Fra-2 regulates HIF-1 $\alpha$  expression in adipocytes [39]. Indeed, our microarray data for Fra-2-regulated genes in melanoma revealed a distinct gene profile compared to breast cancer or T-cell lymphomas [34, 36]. In addition, the decreased ROS levels observed in Fra-2 knockdown melanoma cells are consistent with both the decreased Ero1A expression and accelerated cell cycle transitions, supporting a role for Fra-2 in controlling oxidative stress and the cell cycle progression in melanoma (data not shown) [40]. A subject of ongoing research is whether the decrease in Ero1A expression observed in Fra-2 knockdown melanoma cells is also responsible for the decreased subcutaneous tumor growth in immunocompetent mice via a similar mechanism.

We show that Fra-2 transcriptionally repressed Fam212b expression, which was responsible for the invasive melanoma cell phenotype, cell cycle transition, and angiogenesis in vitro. Interestingly other AP-1 member, notably JunD, can bind Fam212b promoter. JunD is a known regulator of melanoma tumorigenicity, but its interconnection with Fam212b needs further investigations. Moreover, our data did not characterize the mechanism by which Fam212b regulates those phenotypes. Our data support the hypothesis that Fam212b suppress the expression of the serine/threonine kinase PAK4. Consistent with this hypothesis, PAK4 activity acts as a checkpoint during cell cycle progression by controlling CDKN1A expression [41]. Consistently, the *Ccnd1*, *Cdkn1a* and *Fam212b* mRNA are increased in Fra-2 knockdown melanoma cells, which showed an accelerated cell cycle transition in vitro and in vivo. However, when PAK4 is inhibited in the cell lines A375 and A875, the downstream molecular signaling is different, suggesting a



**Fig. 4 Genome-wide profiling of genes and pathways altered in Fra-2 knockdown murine melanoma cells.**

**a** A heatmap of the microarray analysis of the most differentially expressed genes in B16-F0 cells with or without Fra-2 expression using Affymetrix GeneChip® Mouse Transcriptome Assay 1.0. Gene Ontology (GO) and Kyoto Encyclopedia of Genes and Genomes (KEGG) pathway analyses with significant altered 732 genes. Only genes with a fold change greater than 2 and a mean value greater than 7 are shown. **b, c** GO and KEGG pathway analyses of gene enrichment. The top 10 genes and top 5 pathways altered by Fra-2 in the GO analysis (**b**) and KEGG analysis (**c**) are shown. The size of the bars represent in **b** and **c** was a score based on  $-\text{Lg}(p \text{ value})$ . Corrected  $p$  value (FDR)  $\leq 0.05$  for the pathways shown. **d** qPCR validation of Fra-2-regulated genes in Fra-2 knockdown and control B16F0 cells. Graphs present the means for each group and error bars represent the s.e.m.  $P < 0.05$  was considered statistically significant using unpaired Student's  $t$ -tests (two-tailed) for single comparisons.



dependence of the cell line mutation for the action of PAK4. Indeed, A375 is BRAFV600E, while A875 is driven by another mutation. The latest connection that we have highlighted dependent of the Fra-2/Fam212b axis, is the  $\beta$  catenin pathway. It is of particular interest since  $\beta$  Catenin is an important factor for EMT.

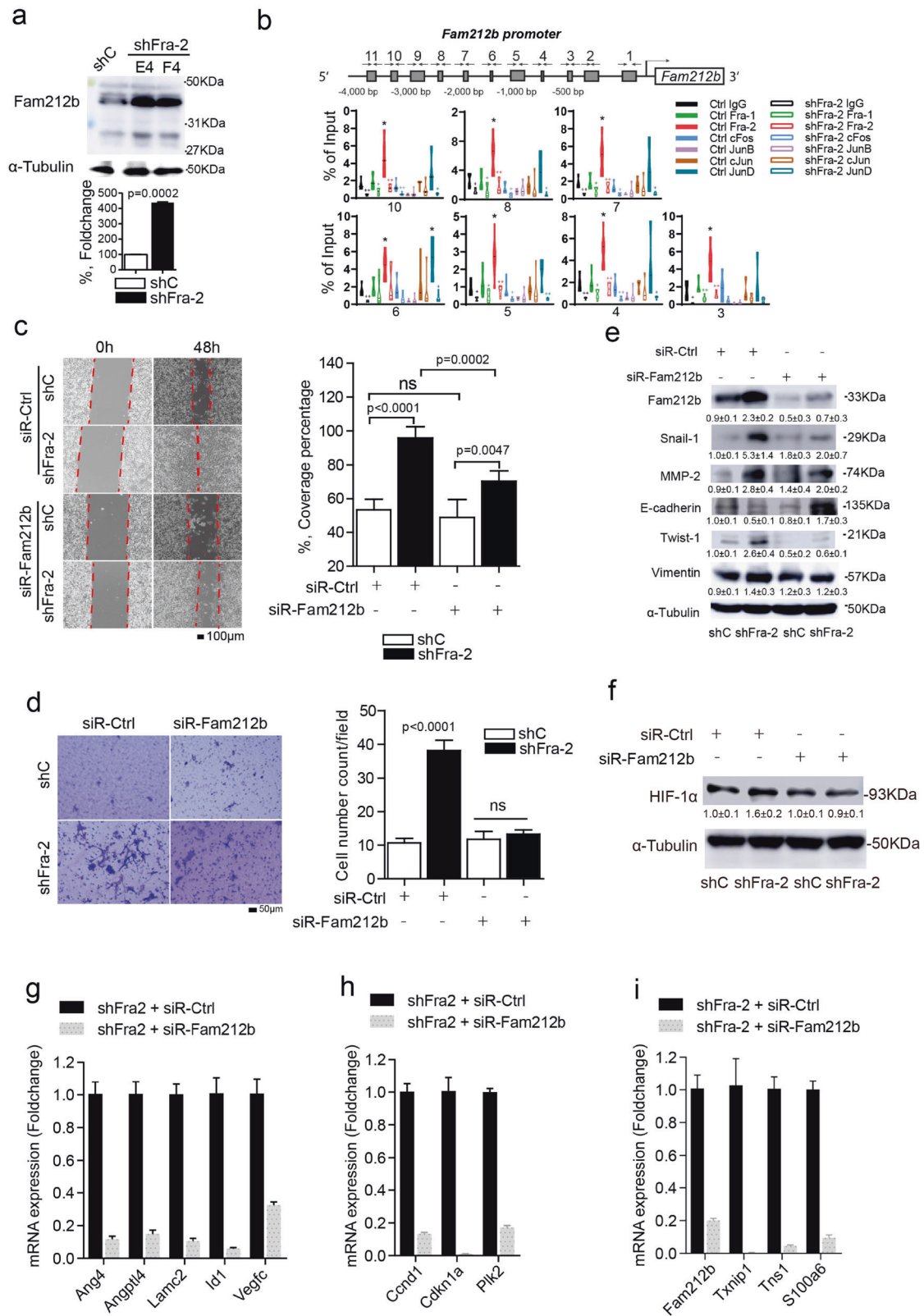
In summary, our data show that Fra-2 deficiency enhances the metastatic process in melanoma cells by inducing metastasis-associated cell cycle transitions, migration, invasion, and angiogenesis. Mechanistically, Fra-2 knockdown transcriptionally regulated Fam212b expression in melanoma. Importantly, downregulation of Fam212b rescued Fra-2KD-induced alterations in melanoma cell migration, invasion, cell cycle transitions, and angiogenesis-related gene expression. Upregulated Fam212b expression was observed in melanomas lymph node metastasis, suggesting that Fam212b might be a new therapeutic target for inhibiting metastasis. These observations not only extend the knowledge on the function of Fra-2/AP-1 transcription factors in the pathogenesis of

melanoma but also defined Fam212b as a new Fra-2 regulated target for melanoma metastasis.

## Methods

### Mouse models

Male C57BL/6 (8–12 weeks old) or BALB/c-nu mice (4–5 weeks old) were purchased from SLAC Laboratory Animal Co., Ltd. (Shanghai, China) and housed in a specific pathogen-free (SPF)-grade animal room with 12 h dark and light cycles. B16-F0 cells were injected into C57BL/6 (8–12 weeks old) or BALB/c-nu mice (4–5 weeks old) for melanoma growth and metastasis studies according to the protocol described by Overwijk et al. [42], with minor modifications. For the subcutaneous melanoma mouse model, B16-F0 cells in 100  $\mu$ l of cold PBS were subcutaneously (s.c.) injected into the flank of BALB/c-nu ( $2.0 \times 10^5$  cells/mouse) or C57BL/6 mice ( $1.0 \times 10^6$  cells/



mouse) using 25 G needles. For the pulmonary metastasis model,  $2.0 \times 10^5$  B16-F0 cells in 250  $\mu$ l of cold PBS were i.v. injected with 27 G needles. For the i.c. injection mouse

model,  $1.0 \times 10^5$  B16-F0 cells in 100  $\mu$ l of cold PBS were directly injected into the left ventricle using 29 G needles. The tumor-bearing mice were monitored every 2–3 days.

◀ **Fig. 5 Fra-2 knockdown-induced effects on melanoma cells depend on Fam212b expression.** **a** Western blot analysis of Fam212b expression in B16-F0 cells after knockdown of Fra-2 with shRNA compared to B16-F0 cells transfected with control vector. Band intensities were quantified with ImageJ software. **b** Model of the putative AP-1 binding sites on *Fam212b* promoter and ChIP analysis of B16-F0 and B16-F0 shFra-2 cell lines. Chromatin was precipitated using anti-Fra-2, anti-Fra-1, anti-cFos, anti-cJun, anti-JunD, anti-JunB or IgG-isotype control antibodies. AP-1 binding was quantified by real-time PCR with primers specific for the putative binding sites, as indicated in the promoter scheme. The Ct values were normalized to the input, and the fold enrichment was calculated by dividing values for the AP-1 pull down by values for the IgG pull down. **c** Representative images and quantification of the migration of B16-F0 and B16-F0 shFra-2 cell lines after transfection with a control siRNA or a siRNA targeting *Fam212b* (Bars: 100  $\mu$ m). **d** Images of crystal violet-stained melanoma cells and quantification of melanoma cells that crossed the BME-coated transwell chamber, which represents the invasion of B16-F0 and B16-F0 shFra-2 cell lines after Fam212b siRNA transfection (Bars: 50  $\mu$ m). **e** Western blot analysis of EMT markers in B16-F0 and B16-F0 shFra-2 cell lines transfected with Fam212b siRNA. Four independent blots were made for E-cadherin; three independent blots were made for snail-1; two independent blots were made for twist-1/2, Fam212b, Vimentin and MMP-2. **f** HIF-1 $\alpha$  proteins in B16-F0 and B16-F0 shFra-2 cell lines transfected with the Fam212b siRNA. Three independent blots were made for HIF-1 $\alpha$  proteins quantification. These blots were stripped and probed according to manufacturer's instructions. No bands represent the same blot. Gene expression analyses of Fra-2 regulated genes (**g**, **i**) and cell cycle genes (**h**) in B16-F0 shFra-2 cell lines transfected with the *Fam212b* siRNA by qPCR. Graphs present the means for each group and error bars represent the s.e.m.  $P < 0.05$  was considered statistically significant using one-way ANOVA (Tukey's multiple comparisons test).

The volumes of the subcutaneous tumors were blindly measured and calculated using the equation length  $\times$  width  $\times$  width/2. No statistical methods were used to estimate sample size. All animal experiments were approved by the ethics committee of Renji Hospital, Shanghai Jiao Tong University School of Medicine.

## Cell cultures

Cells (B16-F0, B16-F1, B16-F10, A375, A875, and SK-Mel-1) were obtained from the Cell Resource Center, Peking Union Medical College (which is the headquarters of the National Infrastructure of Cell Line Resource, NSTI). The cell lines were determined to be free of mycoplasma contamination by PCR and culture. Their species origins were confirmed using PCR. The identity of the cell lines was authenticated with STR profiling (FBI, CODIS). All results can be viewed on the following website: <http://cellresource.cn/>. B16-F0, B16-F1, and SK-Mel-1 cells were cultured in Alpha Minimum Essential Medium ( $\alpha$ -MEM, Life Technologies), whereas A375, A875, and B16-F10 cells were cultured in Dulbecco's Modified Eagle's Medium (DMEM, Life Technologies). All culture media were supplemented with 10% fetal bovine serum (FBS), 100 IU/ml

penicillin and 10  $\mu$ g/ml streptomycin (Gibco<sup>TM</sup>, Life Technologies). All cells were maintained in a 5% CO<sub>2</sub>-humidified atmosphere at 37 °C and passaged at least twice before use in experiments.

## Cell transfection and single-cell clonal assay

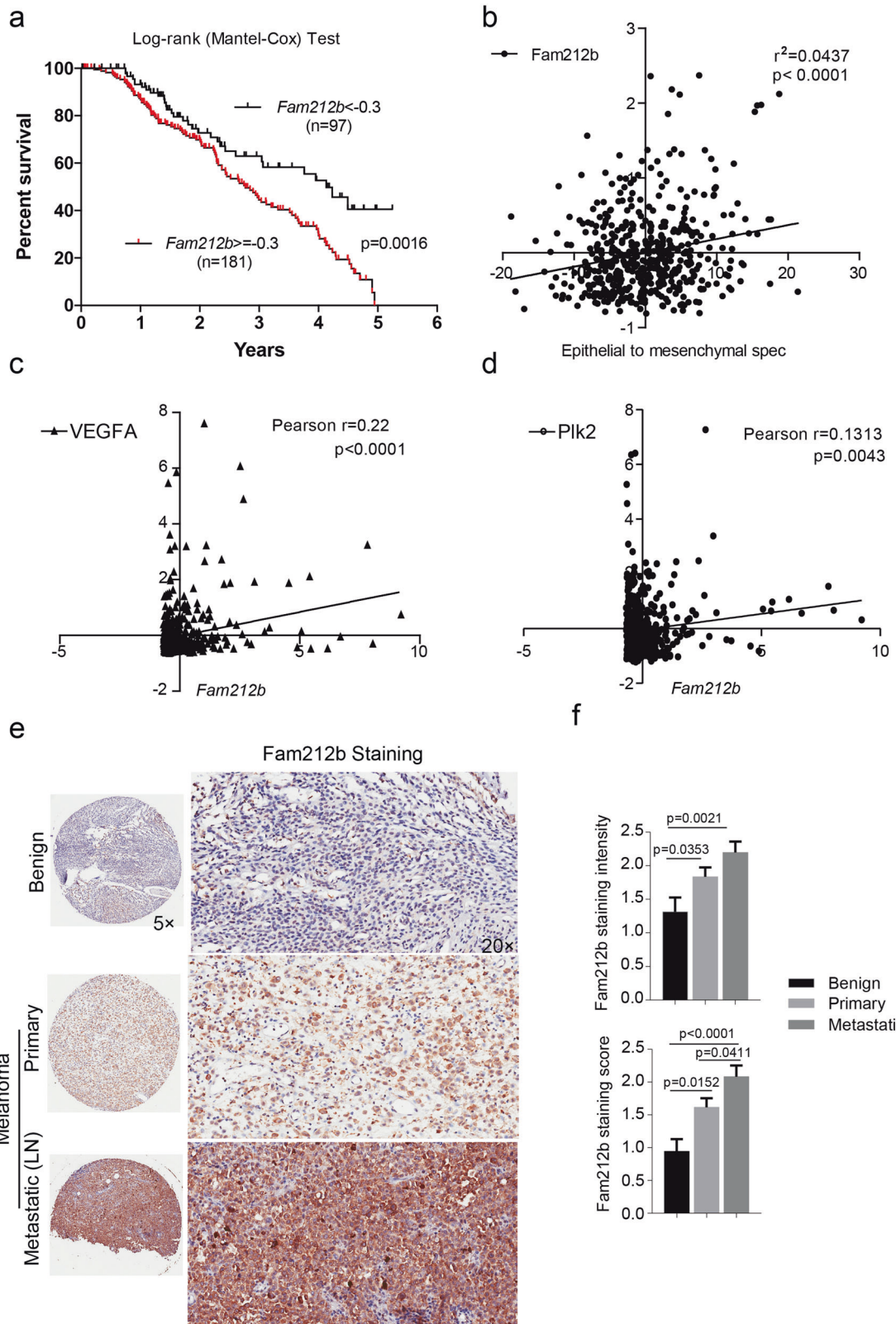
The validated pLKO.1 plasmid vector containing short hairpin RNAs (shRNA) targeting Fra-2 and a puromycin resistance gene and a vehicle vector were purchased from Sigma-Aldrich (MISSION<sup>®</sup> shRNA). The Lipofectamine 3000 transfection reagent (Invitrogen) was used to transfect B16-F0 or A375 and A875 cells with the plasmid, according to the manufacturer's recommendations. The transfected cells were selected with 2  $\mu$ g/ml puromycin (InvivoGen, USA) for 2 weeks. Similarly, A375 and A875 cells were transfected with a plasmid (Biogot Technology, Co., Ltd., Nanjing, China) according to a corresponding transfection protocol, to induce Fam212b overexpression. A serial dilution of  $0.5 \times 10^4$  melanoma cells in 96-well plates was performed to isolate single-cell colonies. Wells containing only one single-cell colony were selected for further analysis. The siRNAs targeting Fam212b (sense: 5'-GGCUAG AUUUACCAGAACUTT-3'; antisense: 5'-AGUUCUGGU AAAUCUAGCCTT-3') and the negative control siRNA were purchased from Genepharma (Genepharma, Inc. Shanghai).

## Cell migration and invasion assay

The scratch assay was performed on six-well plates as described previously [43]. For transwell migration assays,  $1.0 \times 10^5$  B16-F0 cells were seeded in 24-well transwell inserts with an 8  $\mu$ m pore size. For invasion assays,  $4.0 \times 10^5$  B16-F0 cells were seeded in 24-well transwell inserts with 8  $\mu$ m pore size precoated with BME (Trevigen, Cat. #3455-096-02). Serum-free  $\alpha$ -MEM was placed in the upper chamber of the 24-well transwell. After 24–48 h of incubation at 37 °C, the cells that had migrated to the lower side of the insert filter or invaded through the BME were stained with 0.1% crystal violet at the indicated time points. Images were captured from multiple fields using a phase-contrast microscope for analysis.

## Microarray

After Fra-2 KD in B16-F0 cells was confirmed by western blotting, RNA samples were obtained from the Fra-2 KD B16-F0 cells and its control using TRIzol (Invitrogen, USA) and analyzed with the Affymetrix GeneChip<sup>®</sup> Mouse Transcriptome Assay 1.0 at the National Engineering Center for Biochip at Shanghai (Shanghai Biotechnology Corporation, China).



◀ **Fig. 6 Fam212b is a new biomarker for patients with malignant melanoma.** **a** Kaplan–Meier survival curves of patients with melanoma stratified by *Fam212b* mRNA expression levels. Data were obtained from TCGA SKCM samples. Log-rank (Mantel–Cox) test. **b** Analysis of the correlation between the EMT score and *Fam212b* mRNA expression levels in the TCGA SKCM dataset. Pearson's correlation coefficients were used to assess statistical significance.  $EMT\ score = (Fn1 + Vim + Zeb1 + Zeb2 + Twist1 + Twist2 + Snai1 + Snai2 + Cdh2) - (Cldn4 + Cldn7 + Tjp3 + Muc1 + Cdh1)$ . Analysis of the correlation between *Fam212b* mRNA expression levels and *VEGFA* (**c**) or *Plk2* (**d**) mRNA levels obtained from the TCGA SKCM dataset. mRNA expression was determined using a Z-score method. **e** Immunohistochemical staining for Fam212b in paraffin-embedded samples from tissue arrays containing samples from patients with pigmented nevus ( $n = 18$ ) and melanoma ( $n = 82$ ). **f** Analysis of Fam212b staining intensity and score. Staining scores were calculated by multiplying the intensity of Fam212b staining by the percentage of positively stained cells. One-way ANOVA (Tukey's multiple comparisons test) was used to assess the comparison. Graphs present the means for each group and error bars represent the s.e.m.  $P < 0.05$  was considered statistically significant.

### RNA extraction and real-time quantitative PCR

Total RNA was extracted with TRIzol reagent according to the manufacturer's instructions (Invitrogen, USA) and reverse transcribed into complementary DNA using the PrimeScript™ RT reagent Kit with gDNA Eraser (Perfect Real Time) (Takara Biotechnology Co. Ltd., Dalian, China). Quantitative PCR was performed using SYBR® Premix Ex Taq™ II (Tli RNaseH Plus) (Takara Biotechnology Co. Ltd., Dalian, China) on a 7900HT Fast Real-Time PCR System (Applied Biosystems™, Thermo Fisher Scientific Inc., USA).  $\beta$ -Actin was used as a house-keeping gene. All experiments were performed in triplicate and repeated three times. Primer sequences (Supplementary Table 1) were designed and validated by technicians from BioTNT Biotechnologies Co., Ltd. (Shanghai, China).

### Western blot

Cells were scraped and lysed in 2× Laemmli solution (Bio-Rad Laboratories, Inc., USA). Equal amounts of cell lysates were loaded and separated on 8–10% SDS-PAGE gels under denaturing conditions, electro-transferred to 0.2  $\mu$ M polyvinylidene difluoride (PVDF) membranes and then probed with specific primary antibodies (Supplementary Table 2) and secondary antibodies (Beyotime Biotechnology, China). Bands were detected using a BeyoECL Plus chemiluminescence detection kit (Beyotime Biotechnology, China). Images of the bands were obtained using an Amersham™ Imager 600 (GE Healthcare Biosciences; Pittsburg PA).

### Immunohistochemical analysis

The immunohistochemical staining procedure was performed as previously described [43]. All human samples

were obtained after patients provided written informed consent, according to a protocol approved by the ethics committee of Guilin People's Hospital. The pathological tissue sections were stained with antibodies against Fra-2 (Santa Cruz Biotechnology, USA, Cat. # sc-604) at a 1:100 dilution, Fam212b (Sigma-Aldrich Co. LLC, Cat. # HPA027809) at a 1:200 dilution, CD34 (Abcam, USA, Cat. # ab81289) at a 1:100 dilution, or Ki67 (Abcam, USA, Cat. # ab16667) at a 1:200 dilution. The Fra-2 or Fam212b staining scores for tissue slides were calculated by multiplying the nuclear staining intensity (scored from 0 to 4) by the percentage of positive cells, and then divided by 100 in each field. We purchased a tissue array, ME1004e, from Biomax Inc. (USA). Technicians from Shanghai Zuo Cheng Bio Co., Ltd. labeled the sections. Images were acquired using a Nikon Eclipse 80i microscope equipped with a Sony DXC-390P digital camera and NIS-Elements BR2.2 software. Both the percentage of positive cells and the staining intensity of each sample were examined and scored by two independent pathologists who had no knowledge of the patient outcomes.

### ChIP

ChIP experiments were performed with a ChIP-IT Express kit (Active Motif), according to the manufacturer's protocol. Ten micrograms of an anti-AP-1 antibody or a control IgG was used for the immunoprecipitation. Primer sequences and antibody used are listed in Supplementary Table 3.

### Public database analyses

Expression patterns of the Fra-2 gene in diverse human melanoma and normal skin tissues were downloaded from the web-accessible GENT database (Gene Expression database of Normal and Tumor tissues) [17]. The UCSC Cancer Genome Browser (<https://genome-cancer.ucsc.edu>) or the cBioPortal for Cancer Genomics (<http://www.cbioportal.org/index.do>) was used to assess gene expression (mRNA, RNAseq z-scores) from all available patients with skin cutaneous melanoma datasets (Provisional) in The Cancer Genome Atlas (TCGA) [44]. The expression data were graphed using GraphPad Prism 5.0 software (San Diego, CA, USA) and correlated with *Fra-2* mRNA expression or clinical data. The EMT score ((fibronectin 1 (*Fn1*)+vimentin (*Vim*)+zinc finger E-box binding homeobox 1 (*Zeb1*)+*Zeb2* + *Twist1* + *Twist2* + Snail family transcriptional repressor 1 (*Snai1*)+*Snai2* + cadherin 2 (*Cdh2*)-(claudin 4 (*Cldn4*)+*Cldn7* + tight junction protein 3 (*Tjp3*)+mucin 1 (*Muc1*)+*Cdh1*)) was calculated by determining the difference between the expression levels of well-known mesenchymal marker genes and the total

expression levels of known epithelial genes [45]. Higher EMT scores represent a mesenchymal state, whereas lower scores represent an epithelial state [45].

## Statistics

GraphPad Prism 5.0 software was used for statistical analyses; unpaired Student's *t*-tests (two-sided) were used for single comparisons, and one-way ANOVA (analysis of variance) and Tukey's post hoc honest significant difference (HSD) test were used for multiple comparisons, unless indicated otherwise. All data are presented as means  $\pm$  standard errors of the means (s.e.m.) (ns, not significant, \**p* < 0.05, \*\**p* < 0.01, \*\*\**p* < 0.001).

**Acknowledgements** We thank technicians from Shanghai Zuo Cheng Bio Co., Ltd. for providing excellent support for the immunohistochemistry experiments. This study was supported by grants from the Shanghai Science and Technology Committee, Shanghai International Communication Key Project (14430712000, 14430712001, and 14430712002), the National Natural Science Foundation of China (Nos. 81771729, Nos. 81802362, Nos. 81801593), and the Deutsche Forschungs-gemeinschaft (IZKF projekt D23, A01-CRC1181, micro-Bone-SPP1468; BO3811/1-5, BO3811/1-6, BO3811/1-7, and Emmy Noether).

## Compliance with ethical standards

**Conflict of interest** The authors declare that they have no conflict of interest.

**Publisher's note** Springer Nature remains neutral with regard to jurisdictional claims in published maps and institutional affiliations.

## References

- Bhatia S, Tykodi SS, Thompson JA. Treatment of metastatic melanoma: an overview. *Oncol (Williston Park)*. 2009;23:488–96.
- Beaver JA, Theoret MR, Mushti S, He K, Libeg M, Goldberg K, et al. FDA approval of nivolumab for the first-line treatment of patients with BRAFV600 wild-type unresectable or metastatic melanoma. *Clin Cancer Res*. 2017;23:3479–83.
- Caramel J, Papadogeorgakis E, Hill L, Browne GJ, Richard G, Wierinckx A, et al. A switch in the expression of embryonic EMT-inducers drives the development of malignant melanoma. *Cancer Cell*. 2013;24:466–80.
- Li FZ, Dhillon AS, Anderson RL, McArthur G, Ferraro PT. Phenotype switching in melanoma: implications for progression and therapy. *Front Oncol*. 2015;5:31.
- Eferl R, Wagner EF. AP-1: a double-edged sword in tumorigenesis. *Nat Rev Cancer*. 2003;3:859–68.
- Yang S, McNulty S, Meyskens FL Jr. During human melanoma progression AP-1 binding pairs are altered with loss of c-Jun in vitro. *Pigment Cell Res*. 2004;17:74–83.
- Obenauf AC, Zou Y, Ji AL, Vanharanta S, Shu W, Shi H, et al. Therapy-induced tumour secretomes promote resistance and tumour progression. *Nature*. 2015;520:368–72.
- Ramsdale R, Jorissen RN, Li FZ, Al-Obaidi S, Ward T, Sheppard KE, et al. The transcription cofactor c-JUN mediates phenotype switching and BRAF inhibitor resistance in melanoma. *Sci Signal*. 2015;8:ra82.
- Verfaillie A, Imrichova H, Atak ZK, Dewaele M, Rambow F, Hulsemans G, et al. Decoding the regulatory landscape of melanoma reveals TEADS as regulators of the invasive cell state. *Nat Commun*. 2015;6:6683.
- Carro MS, Lim WK, Alvarez MJ, Bollo RJ, Zhao X, Snyder EY, et al. The transcriptional network for mesenchymal transformation of brain tumours. *Nature*. 2010;463:318–25.
- Milde-Langosch K, Janke S, Wagner I, Schroder C, Streichert T, Bamberger AM, et al. Role of Fra-2 in breast cancer: influence on tumor cell invasion and motility. *Breast Cancer Res Treat*. 2008;107:337–47.
- Milde-Langosch K, Bamberger AM, Rieck G, Grund D, Hemminger G, Muller V, et al. Expression and prognostic relevance of activated extracellular-regulated kinases (ERK1/2) in breast cancer. *Br J Cancer*. 2005;92:2206–15.
- Nakayama T, Higuchi T, Oiso N, Kawada A, Yoshie O. Expression and function of FRA2/JUND in cutaneous T-cell lymphomas. *Anticancer Res*. 2012;32:1367–73.
- Yang S, Meyskens FL Jr. Alterations in activating protein 1 composition correlate with phenotypic differentiation changes induced by resveratrol in human melanoma. *Mol Pharm*. 2005;67:298–308.
- Iwasaki Y, Yumoto T, Sakakibara S. Expression profiles of inka2 in the murine nervous system. *Gene Expr Patterns*. 2015;19:83–97.
- Yun CY, You ST, Kim JH, Chung JH, Han SB, Shin EY, et al. p21-activated kinase 4 critically regulates melanogenesis via activation of the CREB/MITF and beta-catenin/MITF pathways. *J Invest Dermatol*. 2015;135:1385–94.
- Shin G, Kang TW, Yang S, Baek SJ, Jeong YS, Kim SY. GENT: gene expression database of normal and tumor tissues. *Cancer Inf*. 2011;10:149–57.
- Barrett T, Wilhite SE, Ledoux P, Evangelista C, Kim IF, Tomashevsky M, et al. NCBI GEO: archive for functional genomics data sets-update. *Nucleic Acids Res*. 2013;41:D991–995.
- Kwong LN, Davies MA. Targeted therapy for melanoma: rational combinatorial approaches. *Oncogene*. 2014;33:1–9.
- Talantov D, Mazumder A, Yu JX, Briggs T, Jiang Y, Backus J, et al. Novel genes associated with malignant melanoma but not benign melanocytic lesions. *Clin Cancer Res*. 2005;11:7234–42.
- Riker AI, Enkemann SA, Fodstad O, Liu S, Ren S, Morris C, et al. The gene expression profiles of primary and metastatic melanoma yields a transition point of tumor progression and metastasis. *BMC Med Genomics*. 2008;1:13.
- Xu L, Shen SS, Hoshida Y, Subramanian A, Ross K, Brunet JP, et al. Gene expression changes in an animal melanoma model correlate with aggressiveness of human melanoma metastases. *Mol Cancer Res*. 2008;6:760–9.
- Rappa G, Fodstad O, Lorico A. The stem cell-associated antigen CD133 (Prominin-1) is a molecular therapeutic target for metastatic melanoma. *Stem Cells*. 2008;26:3008–17.
- Poste G, Doll J, Hart IR, Fidler IJ. In vitro selection of murine B16 melanoma variants with enhanced tissue-invasive properties. *Cancer Res*. 1980;40:1636–44.
- Fidler IJ. Biological behavior of malignant melanoma cells correlated to their survival in vivo. *Cancer Res*. 1975;35:218–24.
- Gene Ontology Consortium. The Gene Ontology (GO) project in 2006. *Nucleic Acids Res*. 2006;34:D322–6.
- Draghici S, Khatri P, Tarca AL, Amin K, Done A, Voichita C, et al. A systems biology approach for pathway level analysis. *Genome Res*. 2007;17:1537–45.
- Baskaran Y, Ang KC, Anekal PV, Chan WL, Grimes JM, Manser E, et al. An in cellulo-derived structure of PAK4 in complex with its inhibitor Inka1. *Nat Commun*. 2015;6:8681.

29. Kappelmann M, Bosserhoff A, Kuphal S. AP-1/c-Jun transcription factors: regulation and function in malignant melanoma. *Eur J Cell Biol.* 2014;93:76–81.
30. Yamanishi DT, Buckmeier JA, Meyskens FL Jr. Expression of c-jun, jun-B, and c-fos proto-oncogenes in human primary melanocytes and metastatic melanomas. *J Invest Dermatol.* 1991; 97:349–53.
31. Smalley KS, Fedorenko IV. Inhibition of BRAF and BRAF +MEK drives a metastatic switch in melanoma. *Mol Cell Oncol.* 2015;2:e1008291.
32. Chiappinelli KB, Strissel PL, Desrichard A, Li H, Henke C, Akman B, et al. Inhibiting DNA methylation causes an interferon response in cancer via dsRNA including endogenous retroviruses. *Cell.* 2017;169:361.
33. Wang J, Sun D, Wang Y, Ren F, Pang S, Wang D, et al. FOSL2 positively regulates TGF-beta1 signalling in non-small cell lung cancer. *PLoS ONE.* 2014;9:e112150.
34. Nakayama T, Hieshima K, Arao T, Jin Z, Nagakubo D, Shirakawa AK, et al. Aberrant expression of Fra-2 promotes CCR4 expression and cell proliferation in adult T-cell leukemia. *Oncogene.* 2008;27:3221–32.
35. Gupta S, Kumar P, Kaur H, Sharma N, Saluja D, Bharti AC, et al. Selective participation of c-Jun with Fra-2/c-Fos promotes aggressive tumor phenotypes and poor prognosis in tongue cancer. *Sci Rep.* 2015;5:16811.
36. Schroder C, Schumacher U, Muller V, Wirtz RM, Streichert T, Richter U, et al. The transcription factor Fra-2 promotes mammary tumour progression by changing the adhesive properties of breast cancer cells. *Eur J Cancer.* 2010;46:1650–60.
37. Tkach V, Tulchinsky E, Lukanidin E, Vinson C, Bock E, Berezin V. Role of the Fos family members, c-Fos, Fra-1 and Fra-2, in the regulation of cell motility. *Oncogene.* 2003;22:5045–54.
38. Hanna SC, Krishnan B, Bailey ST, Moschos SJ, Kuan PF, Shimamura T, et al. HIF1alpha and HIF2alpha independently activate SRC to promote melanoma metastases. *J Clin Invest.* 2013;123: 2078–93.
39. Luther J, Ubieta K, Hannemann N, Jimenez M, Garcia M, Zech C, et al. Fra-2/AP-1 controls adipocyte differentiation and survival by regulating PPARgamma and hypoxia. *Cell Death Differ.* 2014;21:655–64.
40. Deng X, Gao F, May WS Jr. Bcl2 retards G1/S cell cycle transition by regulating intracellular ROS. *Blood.* 2003;102: 3179–85.
41. Nekrasova T, Minden A. PAK4 is required for regulation of the cell-cycle regulatory protein p21, and for control of cell-cycle progression. *J Cell Biochem.* 2011;112:1795–806.
42. Overwijk WW, Restifo NP. B16 as a mouse model for human melanoma. *Curr Protoc Immunol.* 2001;Chapter 20:Unit 20 21.
43. Chen GL, Luo Y, Eriksson D, Meng X, Qian C, Bauerle T, et al. High fat diet increases melanoma cell growth in the bone marrow by inducing osteopontin and interleukin 6. *Oncotarget.* 2016;7:26653–69.
44. Zhu J, Sanborn JZ, Benz S, Szeto C, Hsu F, Kuhn RM, et al. The UCSC cancer genomics browser. *Nat Methods.* 2009;6: 239–40.
45. Salt MB, Bandyopadhyay S, McCormick F. Epithelial-to-mesenchymal transition rewires the molecular path to PI3K-dependent proliferation. *Cancer Discov.* 2014;4:186–99.